TISSUE ENGINEERING: Part A
Volume 19, Numbers 17 and 18, 2013

DOI: 10.1089/ten.tea.2012.0622

Effect of an Inductive Hydrogel Composed of Urinary Bladder Matrix Upon Functional Recovery Following Traumatic Brain Injury

Ling Zhang, PhD,[1] Feng Zhang, PhD,[2] Zhongfang Weng, MD,[2] Bryan N. Brown, PhD,[3] Hongqu Yan, PhD,[4] Xiecheng Michelle Ma, MD,[4] Peter S. Vosler, MD, PhD,[2] Stephen F. Badylak, MD, PhD,[3,5] C. Edward Dixon, PhD,[4] Xinyan Tracy Cui, PhD,[1,3] and Jun Chen, MD, PhD[2]

Traumatic brain injury (TBI) is a major public health problem with no effective clinical treatment. Use of bioactive scaffold materials has been shown to be a promising strategy for tissue regeneration and repair in a number of injury models. Of these scaffold materials, urinary bladder matrix (UBM) derived from porcine bladder tissue, has demonstrated desirable properties for supporting and promoting the growth of neural cells *in vitro*, suggesting its potential as a scaffold for brain tissue repair in the treatment of TBI. Herein we evaluate the biocompatibility of UBM within brain tissue and the effects of UBM delivery upon functional outcome following TBI. A hydrogel form of UBM was injected into healthy rat brains for 1, 3, and 21 days to examine the tissue response to UBM. Multiple measures of tissue injury, including reactive astrocytosis, microglial activation, and neuron degeneration showed that UBM had no deleterious effects on normal brain. Following TBI, the brains were evaluated histologically and behaviorally between sham-operated controls and UBM- and vehicle-treated groups. Application of UBM reduced lesion volume and attenuated trauma-induced myelin disruption. Importantly, UBM treatment resulted in significant neurobehavioral recovery following TBI as demonstrated by improvements in vestibulomotor function; however, no differences in cognitive recovery were observed between the UBM- and vehicle-treated groups. The present study demonstrated that UBM is not only biocompatible within the brain tissue, but also can exert protective effects upon injured brain.

Introduction

Traumatic brain injury (TBI) is a leading cause of death and disability in children and young adults, and it is also a signature injury in the 21th century war veteran.[1] The health care costs associated with the treatment and management of TBI are immense, amounting to ~$60 billion/year.[2] Despite its vast incidence, no viable therapeutic options exist for treatment of TBI.

TBI is thought to induce progressive neurodegeneration characterized by cell loss in specific brain regions.[3] Although endogenous neural stem cells exist,[4] the lack of appropriate cues limits their ability for repair and regeneration. Transplantation of neural stem/progenitor cells showed some promise in promoting neuroprotection and regeneration.[5] However, the survival and functional integration of transplanted cells have been very limited.[6] To address this issue, bioengineered scaffold materials have recently been investigated as a delivery vehicle that can provide controllable external cues, such as cell adhesion signals, soluble trophic factors, and topological, mechanical, or electrical stimuli. A variety of biomaterials have been investigated for implantation into the brain for drug delivery or as a mechanical guiding substrate for wound healing and tissue ingrowth, including degradable polymers and biologically derived materials.[7,8] Among these, the use of biologically active scaffold materials offers the possibility of increasing exogenous neuronal progenitor cell survival, differentiation, and functional integration into the host brain circuitry.[9] Several naturally occurring extracellular matrix (ECM) proteins, such as fibronectin and laminin, have been seeded and transplanted with neural stem cells and results have shown

[1]Department of Bioengineering, University of Pittsburgh, Pittsburgh, Pennsylvania.
[2]Department of Neurology, Center of Cerebrovascular Disease Research, University of Pittsburgh School of Medicine, Pittsburgh, Pennsylvania.
[3]McGowan Institute for Regenerative Medicine, University of Pittsburgh School of Medicine, Pittsburgh, Pennsylvania.
[4]Department of Neurosurgery, University of Pittsburgh, Pittsburgh, Pennsylvania.
[5]Department of Surgery, University of Pittsburgh School of Medicine, Pittsburgh, Pennsylvania.

improved cell survival and functional outcomes, thus demonstrating the beneficial effects of scaffolds.[10]

The ECM of mammalian tissues is a complex mixture of biomolecules that provide three-dimensional physical support and biological signals for cell adhesion, proliferation, and migration. Direct delivery of the ECM has been investigated in preclinical studies and clinical applications in several tissue types, such as esophageal reconstruction, dermal replacement, and vascular conduit (graft) as well as mucosal regeneration with inspiring success.[11] Urinary bladder matrix (UBM), among many kinds of ECMs, is derived from porcine urinary bladder. UBM contains not only the structural molecules present in the ECM such as collagen (mostly type I, but also type III, IV, VI, and VII),[12] fibronectin, laminin, and glycosaminoglycan, but also various growth factors, including vascular endothelial growth factor (VEGF), fibroblast growth factor (FGF), epithelial growth factor (EGF), transforming growth factor-β (TGF-β), kerotinocyte growth factor (KGF), hepatocyte growth factor (HGF), platelet-derived growth factor (PDGF), and bone morphogenetic proteins (BMP).[13–16] Neurons grow well and extend long neurites on the surface of UBM, while Schwann cells migrate toward the degradation products of UBM in a concentration-dependent manner *in vitro*.[17] The preparation and rheology of the UBM hydrogel have also been studied. Due to the tunable mechanical property of the UBM hydrogel, UBM is suitable for application as an injectable material for soft tissue reconstruction.[18]

These findings suggest that UBM alone is a candidate material for cell therapy in the brain. However, the use and evaluation of UBM material in brain tissue has not yet been reported. Therefore, the primary goal of this study was to assess the brain tissue response to injection of UBM. Additionally, the degradation products of UBM scaffolds promote migration and proliferation of multipotential progenitor cells to sites of tissue injury as well as inhibit both chemotaxis and proliferation of differentiated endothelial cells. These activities may play an important role in the *in vivo* recruitment of endogenous neural stem cells to the site of healing, thereby promoting tissue healing.[19] Further, the various growth factors found within ECM scaffold materials, such as VEGF and TGF-β, are known to provide neuroprotective or anti-inflammatory effects in the brain.[20,21] Based on this knowledge, we hypothesized that UBM may be capable of inducing biological responses favorable to tissue repair after TBI.

Materials and Methods

Preparation of UBM solution

UBM powder was obtained as previously described.[18] Briefly, porcine urinary bladders were harvested from 6-months-old pigs weighing ~108–118 kg (Thoma Meat Market) immediately following euthanasia. First, the excess connective tissue and residual urine were removed. The tunica serosa, tunica muscularis externa, the tunica submucosa, and majority of the tunica muscularis mucosa were then mechanically removed. The luminal surface was soaked with a 1.0 N saline solution to dissociate the urothelial cells of the tunica. The resulting biomaterial, which was composed of the basement membrane of the urothelial cells plus the subjacent lamina propria, was referred to as UBM. UBM sheets were placed in a solution containing 0.1% (v/v) peracetic acid (Sigma), 4% (v/v) ethanol (Sigma), and 95.9% (v/v) sterile water for 2 h. To remove peracetic acid residue, two 15-min phosphate-buffered saline (PBS; pH = 7.4) washes were introduced, followed by two 15-min washes with sterile water. The decellularized UBM sheets were then lyophilized using an FTS Systems Bulk Freeze Dryer Model 8–54. Enzymatic degradation products were generated as previously described.[18] Briefly, lyophilized scaffold materials were powdered using a Wiley mill and filtered through a 40 mesh screen. The powdered material was solubilized at a concentration of 10 mg/mL in a solution containing 1.0 mg/mL pepsin in 0.01 N HCl at a constant stir rate for 48 h. The ECM digest solution was then frozen at −20°C until use in subsequent experiments. Enzymatic digestion was stopped by raising the pH of the solution to 7.4 using NaOH and diluting the solution to the desired concentration with PBS before further testing. In the present study, the material was diluted to a final concentration of a 5 mg/mL solution at 4°C. All solutions were kept at 4°C before and after being mixed together by vortex to prevent gelling. The mixed solution was centrifuged at 1000 rpm for 2 min to eliminate bubbles before injection.

Animals and surgical procedures

All studies carefully conformed to the guidelines outlined in the Guide for the Care and Use of Laboratory Animals from the NIH Department of Health and Human Services and were approved by the University of Pittsburgh Medical Center Institutional Animal Care and Use Committee. Male Sprague-Dawley rats (Harlan Laboratories) weighing 250–300 grams on the day of surgery were used. Rats were group-housed (two per cage) in standard steel/wire mesh cages at room temperature (22°C ± 2°C) under standard 12-h light/12-h dark cycles with free access to food and water. These rats were used for two purposes: uninjured rats to evaluate tissue reactions to UBM and controlled cortical impact (CCI) injured rats in the TBI model. Three animals per time point (1d, 3d, 21d) were sufficient to evaluate the morphologic central nervous ystem (CNS) tissue response to the presence of the UBM hydrogel. For the TBI experiment, 6 rats in the sham group and 10 rats in the vehicle (PBS) group were sufficient since they were very consistent in resulting behavior and the same as our previous studies. Twelve rats received UBM treatment after CCI injury to determine the effect of UBM following TBI.

Injection of UBM solution into uninjured brain

All rats were anesthetized initially with 4% isoflurane with a 2:1 N_2O/O_2 mixture in a vented anesthesia chamber. Following endotracheal intubation, rats were ventilated mechanically with a 1%–1.5% isoflurane mixture. Animals were mounted in a stereotaxic frame on the injury device in a prone position secured by ear and incisor bars. The head was held in a horizontal plane with respect to the interaural line. A midline incision was made, the soft tissues reflected, and a 7-mm-diameter craniotomy was made between lambda and bregma and centered 5 mm lateral of the central suture. Core body temperature was monitored continuously by a rectal thermistor probe and maintained at 37°C ± 0.5°C with a heating pad. A 5 μL UBM solution was injected using a 10-μL Hampton syringe into the dorso-plus ventrolateral or laterodorsal thalamic nucleus area beneath CA3 of hippocampus

in the right cerebral hemisphere, and 5 μL of PBS (vehicle) was injected to the contralateral side by a syringe at 0.5 μL/min controlled by a Micro 4 Microsyringe Pump Controller (World Precision Instruments). The injection lasted for 10 min and was held for 30 min to allow the solution to gel before needle withdrawal. The host tissue response to the UBM hydrogel and the cytotoxicity of the UBM hydrogel to the brain was then examined after 1, 3, and 21 days with an $n = 3$ for each group. After 1, 3, and 21 days, rats were sacrificed and brain tissue was prepared for immunolabeling and FluoroJade B staining as described below.

Experimental injury model: CCI

The CCI injury device[22] consisted of a small (1.975 cm) bore, double-acting, stroke-constrained, pneumatic cylinder with a 5.0-cm stroke. The cylinder was rigidly mounted in a vertical position on a crossbar, which could be precisely adjusted in the vertical axis. The lower rod end had an impactor tip (6 mm diameter) attached (i.e., the part of the shaft that comes into contact with the exposed dura mater). The upper rod end was attached to the transducer core of a linear velocity displacement transducer (LVDT). The velocity of the impactor shaft was controlled by gas pressure. The impact velocity was measured directly by the LVDT (Shaevitz Model 500 HR; Macro Sensors), which produced an analog signal that was recorded by a PC-based data acquisition system (Axoscope; Axon Instruments, Inc.) for analysis of time/displacement parameters of the impactor.

All rats were anesthetized and subjected to the same preparation as uninjured rats. The same brain area on the right hemisphere was exposed as described above. The animals received a cortical impact through the right craniotomy at a velocity of 4 m/s. The injury device was set to produce a tissue deformation of 2.6 mm. Sham rats were subjected to identical surgical procedures, but did not receive a cortical impact. The sham rats were used as control for nonspecific methodological effects (such as those due to anesthesia and surgery). The core body temperature was monitored continuously by a rectal thermistor probe and maintained at 37°C ± 0.5°C with a heating pad. After injury, rats were housed in separate cages from uninjured animals.

Injection of UBM solution into injured brain

One day following CCI injury, all rats were anesthetized and placed in a stereotaxic platform. The surgical site was reopened. The injury site was exposed and a 5 μL solution (PBS or UBM) was injected into the CA3 field of ipsilateral hippocampus following the same injection procedure as 2.3.1. Experimental groups consisted of sham-operated controls ($n = 6$) and UBM- ($n = 10$) and vehicle- ($n = 12$) treated rats following TBI. After 21 days, rats were sacrificed and brain tissue was prepared for further tissue analysis as described below. Alternatively, the rats also underwent behavioral testing following TBI as outlined below.

Tissue preparation

Twenty-one days postinjury, animals were sacrificed. Tissue preparation procedures were as previously reported.[23] Briefly, animals were deeply anesthetized with pentobarbital (Nembutal, 80–100 mg/kg; Abbott Laboratories) and were transcardially perfused with 100 mL 0.1 M PBS with 50 U/mL heparin (pH 7.4), followed by 500 mL 4% paraformaldehyde with 15% saturated picric acid in a 0.1 M phosphate buffer (pH 7.4). After perfusion, the brain was removed and placed into the same fixative for 30 min, and then immersed in 4% paraformaldehyde in a 0.1 M phosphate buffer (pH 7.4) at 4°C overnight. The brain was transferred to 15% sucrose in a 0.1 M phosphate buffer (pH 7.4) at 4°C for 24 h, and then to 30% sucrose in a 0.1 M phosphate buffer pH 7.4 at 4°C until the brain was sunk. The cryoprotected rat brain was frozen and used for microtome sectioning. Coronal sections were cut in 35-μm thickness in a microtome (HM550 sliding microtome) and collected in 24-well culture plates contained with a stocking solution, which enables the long-term preservation of these sections.

Immunofluorescence of GFAP and Iba-1 staining

Immunofluorescence for GFAP and Iba-1 were conducted in 24-well culture plates by the free floating technique Sections were pretreated with 3% H_2O_2 in methanol for 10 min at room temperature, and blocked with 10% normal goat serum (NGS) and 0.1% Triton X-100 in 0.1 M PBS. Sections were incubated with the rabbit anti-GFAP (1:500; Dako), rabbit anti-Iba-1 (1:500; Wako), and mouse anti-nestin (1:1000; BD Biosciences) antibodies with 5% NGS and 0.1% Triton X-100 in 0.1 M PBS at 4°C for 16–24 h. Then, sections were incubated with the Alexa 488 (1:500) goat anti-rabbit or goat anti-mouse secondary antibody with 5% donkey serum for 2 h at 4°C. Sections were rinsed several times in 0.1 M Tris-buffered saline (TBS), mounted on subbed slides, and dry at room temperature. After drying, slides were rinsed with DD-H_2O and coverslipped with an antifade mounting medium (fluoromount-G; Southern Biotech).

FluoroJade B staining

The sections were mounted on 2% gelatin-coated slides, and then air-dried on a slide warmer at 50°C for at least half an hour. The slides were first immersed in a solution containing 1% sodium hydroxide in 80% alcohol (20 mL of 5% NaOH added to 80 mL absolute alcohol) for 5 min. This was followed by 2 min in 70% alcohol and 2 min in distilled water. The slides were then transferred to a solution of 0.06% potassium permanganate for 10 min, preferably on a shaker table to insure consistent background suppression between sections. The slides were then rinsed in distilled water for 2 min. The staining solution was prepared from a 0.01% stock solution for Fluoro-Jade B (Millipore) that was made by adding 10 mg of the dye powder to 100 mL of distilled water. To make up 100 mL of the staining solution, 4 mL of the stock solution was added to 96 mL of 0.1% acetic acid vehicle. This results in a final dye concentration of 0.0004%. The stock solution, when stored in the refrigerator was stable for months, whereas the staining solution was typically prepared within 10 min of use and was not reused. After 20 min in the staining solution, the slides were rinsed for 1 min in each of three distilled water washes. Excess water was removed by briefly (about 15 s) draining the slides vertically on a paper towel. The slides were then placed on a slide warmer, set at ~50°C, until they were fully dry, (e.g., 5–10 min). The dry slides were cleared by immersion in xylene for at least a minute before coverslipping with Cytoseal XYL (Thermo Fisher).

Hematoxylin and eosin staining and lesion volume measurement

Hematoxylin and eosin (H&E) staining was done to reveal histological or pathological morphology changes. The floating serial coronal sections of TBI rats were selected and spread onto colorfrost/plus slides (Fisher Scientific). After drying under the hood, they were stained with H&E. For lesion volume measurement, six brain sections from each rat were traced by a microcomputer imaging device (Imaging Research), as previously described.[24] The lesion area on each section (A_i) was calculated (i.e., the intact area of the ipsilateral hemisphere is subtracted from the area of the contralateral hemisphere[25]) and the lesion volume was obtained by multiplying lesion areas with the distance of the sections. Then, the volumes were added together to get a final volume across certain distance from anterior to posterior, shown in formula (1). The lesion volume was finally presented as a volume percentage of the lesion compared with the contralateral hemisphere, shown in formula (2).

$V_L = \sum_{i=1}^{n} A_i \times d$, ($V_L$ is the lesion volume across certain distance; A_i is the lesion area on each section; n represent the number of slides) (1)

Lesion volume% $= \frac{V_L}{V_C} \times 100\%$, ($V_C$ is the corresponding volume in contralateral hemisphere) (2)

Immunolabeling for myelin basic protein and immunofluorescence staining

Immunolabeling for the myelin basic protein (MBP) was conducted in 24-well culture plates by the free-floating technique. Sections were preblocked with 10% NGS and 0.1% Triton X-100 in 0.1 M PBS. Sections were incubated with the mouse anti-MBP (1:500; Millipore) antibody with 5% NGS and 0.1% Triton X-100 in 0.1 M PBS at 4°C for 16–24 h. Affinity-purified goat anti-mouse IgG conjugated with peroxidase (1:50; Jackson ImmunoResearch Laboratories) were incubated as secondary antibodies with 5% normal serum and 0.1% Triton X-100 in 0.1 M PBS at 4°C for 2 h on a shaker. Tissue sections were rinsed between all steps with 0.1% Triton X-100 in 0.1 M PBS three times for at least 5 min each time. The peroxidase reaction was developed by a DAB Substrate Kit (Vector) until a dark brown reaction product was evident. Sections were rinsed several times in 0.1 M TBS, mounted on subbed slides, dehydrated in alcohols, defatted in xylenes, and coverslipped with Cytoseal XYL (Thermo Fisher) for light microscopic analysis.

Brain sections were first blocked with 10% NGS in the 0.1 M PBS solution for 1 h, and then incubated with the mouse monoclonal antibody recognizing the nonphosphorylated neurofilament H (SMI32, 1:250; Covance) and the rabbit antibody recognizing the MBP-1 antibody (1:250; Millipore) in a 5% NGS/PBS solution at 37°C each, and then at 4°C overnight for 1 h. The next day, sections were washed with PBS for three times and incubated in a mixture of the anti-mouse secondary antibody-conjugated with DyLight™ 594 (Jackson ImmunoResearch Laboratories) and the anti-rabbit secondary antibody conjugated with DyLight™ 488 (Jackson ImmunoResearch Laboratories) at 37°C for 1 h. Subsequently, the sections were placed on glass slides and coversliped with the VECTASHIELD mounting medium containing DAPI (Vector Laboratories, Inc.) before confocal fluorescence microscopy (FV1000; Olympus).

Behavioral testing

Vestibular motor function (days 1–5). Gross vestibulomotor function was assessed on a beam-balance task that consisted of placing the animal on a suspended, narrow wooden beam (1.5 cm wide) and a buffer recording the duration it remained on the beam for a maximum of 60 s. Training before injury consisted of three trials, during which, baseline measurements were taken. Since the rats will gradually recover their motor function after 5 days in this model, behavior only during the first 5 days were assessed.

More complex vestibulomotor functions and coordination were assessed using a modified beam-walking task. Briefly, this task consisted of training rats to escape a bright light and high-decibel white noise (Model #15800C; Lafayette Instruments, Inc.) by traversing a narrow wooden beam (2.5 × 100 cm) and entering a darkened goal box at the opposite end. Noxious stimuli were terminated when the rat entered the goal box. Four pegs (3.0 mm diameter, 4.0 cm high) were placed in an alternating sequence along the beam to increase the difficulty of the task. The performance was assessed by the latency to traverse the beam. If the rat traversed the beam and entered the box, a score of 5 was recorded. If the rat fell, the score correlating to the point of peg from which the rat fell was recorded. Data for each session consisted of the mean of three trials. All rats were pretrained before injury.

Cognitive function

A Morris water maze task variant was used to compare acquisition rates between groups. The maze consisted of a plastic pool (180 cm in diameter and 60 cm in depth) filled with water to a depth of 28 cm with a clear Plexiglas stand (10 cm in diameter and 26 cm high, i.e., 2 cm below the water's surface) used as the hidden goal platform. The pool was located in a 2.5 × 2.5-m room with numerous extramaze cues (e.g., posters) that remained constant throughout the experiment. Water maze testing began on day 14 postinjury to avoid possible confounds with the motor deficits observed in the first few days after injury. The rats were given four trials per day for 5 consecutive days to assess the performance. For each daily block of four trials, the subjects were placed in the pool facing the wall. Trials were initiated from each of the four possible start locations (north, east, south, or west) in a randomized manner. The goal platform was positioned 45 cm from the outside wall and was placed in the northeast, southeast, southwest, or northwest quadrant of the maze. The location of the platform was held constant for each animal. A maximum of 120 s was allowed to each rat to find the hidden platform. If the rat failed to find the platform within the allowed time, it was placed on the platform by the experimenter, where it remained for 30 s before being placed in a heated incubator between trials (a 4-min intertrial interval).

Statistical analysis

Data are expressed as the mean ± standard error of the mean. Comparisons of lesion areas and neurobehavioral tests were performed with analysis of variance and Fisher's *post hoc* tests. Trend analysis was performed for behavior results by regression analysis to extract the trend of behavior along with time. A significance level of $p < 0.05$ was used for all tests.

Results

Brain tissue is compatible with UBM

We first attempted to determine if there was an endogenous inflammatory or neurotoxic effect of the UBM hydrogel on a normal rat brain. Staining for Iba-1, a microglial-specific protein upregulated following microglial activation, revealed activated microglia along the needle track and injection site at 1 and 3 days. Because there were activated microglia in both injection sides, it is deduced to be a typical acute inflammatory response in response to the injection injury. At day 21, microglia activation had subsided. At all time points, the number and spatial distribution of activated microglia did not show an obvious difference between the vehicle (PBS) and treatment (UBM) groups (Fig. 1a, b).

To determine if implantation of the UBM hydrogel resulted in reactive astrocytosis, we next measured GFAP immunoreactivity in PBS- and UBM-treated brains. In both groups, there is a large zone of enhanced GFAP staining at the injection site initially. The intensity decreased at day 3 and by day 21, the fluorescence is only seen on the surface of the brain. No marked astrogliosis was found in either the PBS- or UBM-injected areas. Such response is consistent with what is known as an acute needle insult. The lack of an astrocytic scar at the injection site of the UBM suggests rapid degradation and good biocompatibility of the material (Fig. 1c, d).

Finally, we used FluoroJade B staining to detect degenerating neurons following UBM treatment. Our results did not show any difference between the treatment and the vehicle groups at any time point (Fig. 1e). A similar number of degenerating neurons were observed at the injection sites on both sides at day 1, likely due to injection-induced injury. However, no FluoroJade B-positive cells were found at later time points. Overall, our data demonstrate that UBM injected in the brain does not cause an overt inflammatory reaction via microglial activation, astrocytosis, or neurodegeneration.

Lesion volume is diminished following UBM treatment

The primary hypothesis of the present work was that the UBM hydrogel would provide a scaffold for cell survival, migration, or proliferation to more effectively repair the injured area following TBI. We therefore examined if injection of UBM hydrogel had an effect on TBI-induced lesion volume. As expected, the lesion volume was minimal in sham-treated rats (5.38% ± 4.43%). TBI, however, caused a large tissue deficit (41.32% ± 4.59%) that was markedly reduced in UBM-treated rats (24.34% ± 3.59%) (Fig. 2). The examination of neuronal counts in the hippocampal CA3 field, however, revealed no significant decrease in CA3 neuronal death in UBM hydrogel-injected rats compared to

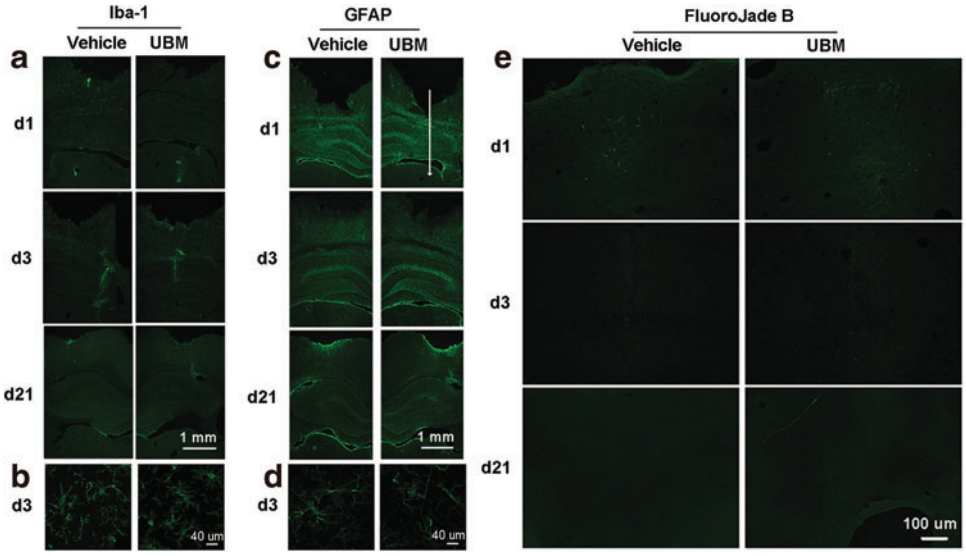

FIG. 1. Urinary bladder matrix (UBM) injection does not activate microglia, does not cause astrocytosis or neurodegeneration. **(a, b)** There was no discernable increase in expression of the microglia, or astrocyte activation indicator Iba-1 or GFAP, as measured by immunofluorescent staining between UBM- and vehicle-treated cerebral hemispheres. The representative images shown here are the tissue regions from the needle track to the injection site. The white arrow indicates the needle track and the tip of the arrow is the injection site. Note the increased number of activated microglia along the needle track at day 3, which subsided by day 21 in both UBM- and vehicle-treated hemispheres. Histological sections are representative of the findings from both hemispheres with an $n = 3$ rats per time period. **(c, d)** Immunofluorescent staining for GFAP presented little difference between UBM- and phosphate-buffered saline (PBS)-injected brain tissue after 1, 3, and 21 days. $n = 3$ rats per time period at 1, 3, and 21 days following injection. **(b, d)** High magnification of the images at day 3 shows the morphology of activated microglia and astrocytes near the injection site of both groups. **(e)** Staining UBM- and vehicle-injected brain sections with the neurodegeneration marker FluoroJade-B indicates that UBM treatment does not result in more degenerative neurons than control (PBS injection). There was a slight presence of degenerative neurons around the tip of injection on day 1 after injection, but this was equal between UBM- and vehicle-treated hemispheres. Histological sections are representative of the findings from both hemispheres with an $n = 3$ rats per time period. Scale bar: 1 mm in **(a, c)**; 40 μm in **(b, d)**; 100 μm in **(e)**. Color images available online at www.liebertpub.com/tea

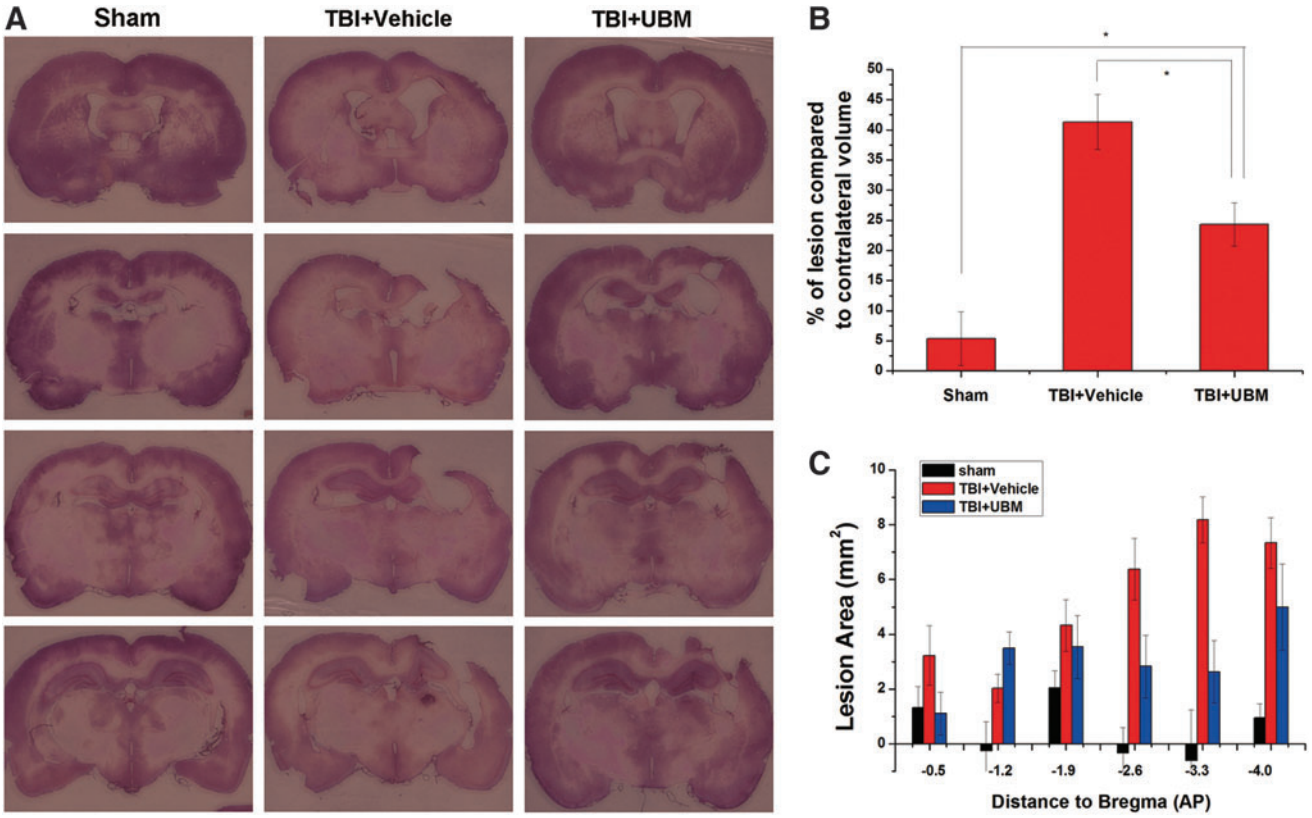

FIG. 2. UBM treatment decreases the traumatic brain injury (TBI)-induced lesion area. **(A)** Representative hematoxylin and eosin-stained coronal sections near the injury epicenter from sham-operated, vehicle-, and UBM-treated rats 21 days following TBI. These sections are examples from three different treated animals at the anterior to posterior (AP) coordinates with respect to bregma (top to bottom). **(B)** The percentage of lesion volume compared to contralateral volume was significantly decreased in UBM- compared to vehicle-treated rats. Of note, UBM-treated rats had a significantly increased lesion volume compared to sham-operated controls. **(C)** Examination of the distribution of lesion showed that the tissue was mainly spared at around AP −2.6 to −4.0 mm in the UBM-treated group. Bars represent mean ± standard error (SE) with an $n = 6$, 10, and 12, for sham-, UBM-, and vehicle-treated groups, respectively. Scale bars: 5 mm. *$p < 0.05$. Color images available online at www.liebertpub.com/tea

vehicle-treated controls (data not shown). Overall, the reduction in lesion volume is an important finding as it confirmed our initial hypothesis that the UBM hydrogel can provide a significant scaffold to protect or repair injured brain.

UBM decreases white matter injury

In addition to the UBM hydrogel having an overall mass-restoring effect on the injured brain, we examined the effect of UBM injection on white matter injury, another contributing factor of TBI-induced brain injury. MBP is widely expressed on axons, and therefore, loss or rearrangement of MBP is a measure of white matter injury.[26] Distribution and arrangement of MBP within samples from each group was revealed by immunolabeling studies. The brown, long tract or round islands showed the arrangement of MBP. The extent of the disorganization of MBP differed among the three experimental groups. Rats who received TBI and PBS showed a severely disrupted arrangement of MBP in the striatum, indicating extensive injury to white matter (Fig. 3A). Rats treated with UBM also showed derangement of MBP compared to sham control; however, the extent of derangement was less compared to vehicle-treated rats. The disarrangement also happened in corpus callosum. Rats treated with the UBM hydrogel showed less derangement than rats treated with vehicle.

White matter injury can also be assessed by the staining of SMI32 and MBP in the striatum around the CCI lesion, as indicated in Figure 3C. In the striatum (Fig. 3B), a sharp increase in SMI32 in rats treated with vehicle was observed, compared to sham. Concomitantly, a decrease in MBP staining was observed in rats treated with vehicle. A decrease in SMI32 in rats treated with the UBM hydrogel was observed compared to that in rats treated with vehicle. And an increase in MBP staining was observed, indicating reduced white matter injury.

SMI32 and MBP staining intensities from a minimum of 6 images of the striatum were averaged, thus, the SMI32/MBP ratio was determined. The relative SMI32/MBP ratio was substantially higher in rats treated with vehicle than sham, indicating increased white matter injury. A significantly lower SMI32/MBP ratio was observed in rats treated with the UBM hydrogel than with vehicle, suggesting that the UBM hydrogel can attenuate CCI-induced white matter injury (Fig. 3D). Thus, in addition to having a decreased lesion volume, rats that received UBM injection also had decreased white matter damage following TBI.

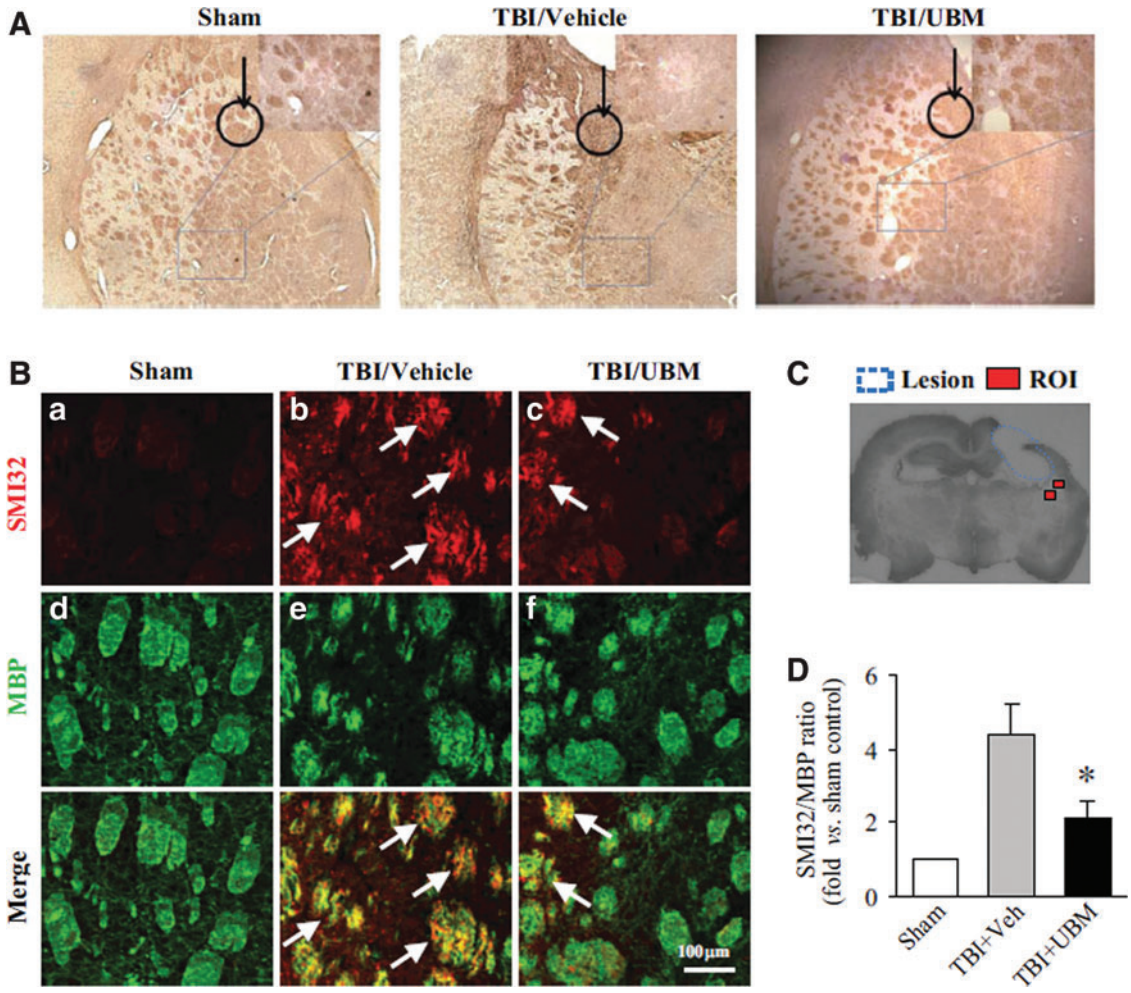

FIG. 3. UBM treatment attenuates white matter injury in rats following TBI. **(A)** Staining for the myelin basic protein (MBP) following TBI as an indication of white matter damage revealed that TBI results in a high degree of disorganization of myelin in the rat striatum compared to sham. UBM injection following TBI attenuated the disruption of myelin organization. The black circle with an arrow in each image indicates the implantation position, in the striatum right beneath the CA3 area. The white matter tract underneath the implantation site was observed and shown in the magnified image. **(B)** Immunofluorescent staining of SMI32 and BMP showed that an increase in SMI32 and a decrease in MBP in rats following TBI compared with sham, but a decrease in SMI32 and an increase in MBP staining was observed in rats treated with UBM compared with treated with vehicle, indicating that UBM injection reduced white matter injury. Arrows indicate the increased SMI132 immunofluorescence in the bundles in the TBI striatum. **(C)** The location of regions of interest (ROI) in the striatum around lesion are indicated as red squares, where the SM132/MBP ratio was calculated 21 days following TBI. **(D)** The SMI32/MBP ratio indicates the extent of white matter injury. The relative SMI32/MBP ratio was decreased in rats treated with UBM compared to vehicle treatment. Images are representative of staining for MBP and SMI32 in sham- ($n=6$), vehicle- ($n=12$), and UBM-treated ($n=10$) groups at 21 days after TBI. Data are presented as mean ± SE, $^*p<0.05$ versus vehicle or UBM. Color images available online at www.liebertpub.com/tea

Improved vestibulomotor performance with UBM treatment

An important parameter for determining if an intervention has a potential for therapeutic efficacy is to examine neurobehavioral recovery. Our results in the previous section showed decreased disorganization of MBP in the striatum upon UBM injection, which is a neuroanatomical area associated with motor function. Therefore, we used a test of vestibulomotor performance to determine if UBM treatment provided an improved functional outcome following TBI. TBI resulted in decreased vestibulomotor function as demonstrated by a decreased duration on the balance beam, an increased latency to traverse the beam, and a decreased composite score of vestibulomotor performance (Fig. 4). Treatment with UBM significantly improved the performance on the beam balancing test on all the aforementioned metrics compared to vehicle-treated rats after TBI. Of note, at 5 days post-TBI, the balance time of UBM-treated rats was indistinguishable from sham-operated controls (Fig. 4A).

Last, we evaluated the cognitive performance using the Morris water maze test to determine if UBM treatment could improve the cognitive outcome after TBI. This test measures spatial learning and memory, functions that are impaired following TBI.[27] The latency to locate the submerged platform from day 14 to 18 for the sham group was significantly shorter than those of both the vehicle-treated and UBM-treated groups. The UBM treatment did not improve the

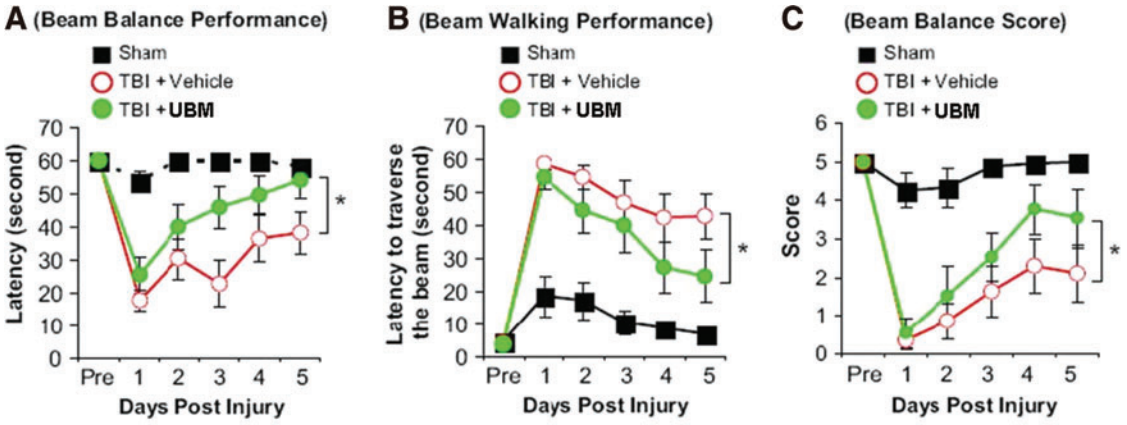

FIG. 4. Implantation of the UBM scaffold reduced motor deficits in the controlled cortical impact (CCI) model of TBI. Injection of the UBM scaffold (5 μL) was performed at 24 h after CCI, and motor functions were evaluated 1–5 days after CCI. The graphs illustrate the quantitative analysis of the beam balance performance **(A)**, beam walking performance **(B)**, and beam balance score **(C)** among the 3 groups of rats. Data are mean ± SD, $*p < 0.05$ between TBI + vehicle and TBI + UBM groups. Color images available online at www.liebertpub.com/tea

cognitive performance relative to vehicle treatment following TBI as there was no significant difference in latency to reach the platform between the groups (Fig. 5). Taken together, these experiments demonstrate that the benefits of UBM hydrogel treatment on neurobehavioral recovery are relegated to specific functions.

Discussion

The present study examined the effects of biologic scaffold hydrogel injection into the brain. Results showed that the ECM derived from the urinary bladder (UBM) has elicited no adverse inflammatory response within rat brain tissue, lessens tissue damage following experimentally induced TBI, and promotes motor functional recovery. However, no improvement in the cognitive performance of UBM-injected TBI rats was observed.

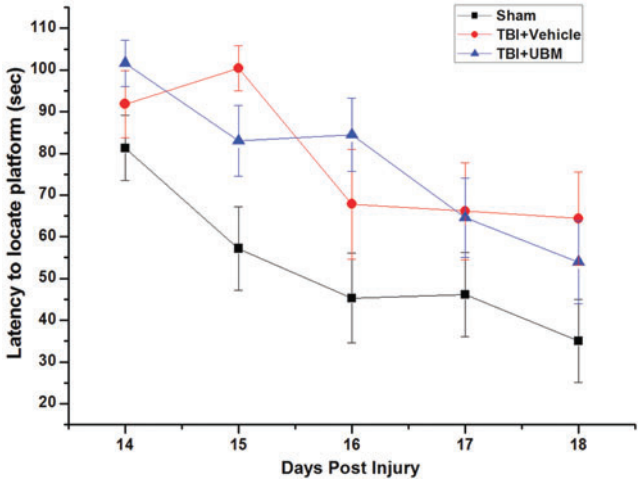

FIG. 5. Spatial learning function of rats received UBM implantation following TBI was not improved by studies from the Morris water maze. Spatial learning function was evaluated 14–18 days after CCI. The graphs illustrate the quantitative analysis of latency to locate the platform. There is no significant difference among the three groups of rats. Data are mean ± SD. Color images available online at www.liebertpub.com/tea

The ECM has been extensively investigated in biomedical applications and many types of ECM-based scaffold materials have already been approved for clinical use.[11] The most extensively studied ECM is small intestinal submucosa (SIS) prepared from porcine sources. SIS has been used in more than four million patients to date for reconstruction of various types of tissues, including the body wall, rotator cuff, urinary bladder, urethra, ureter, and esophagus. Despite being derived from porcine sources, there is strong evidence that adverse immune response events do not occur[28] and in fact, a shift to a regulatory and constructive M2 macrophage phenotype has been repeatedly shown.[29,30] Schwartz has suggested that a prominent M2 phenotype presence after brain injury is critical for constructive remodeling outcomes.[31–33] It is plausible that these properties may be generalized to other types of ECM materials, including ECM materials recently identified from CNS tissue.[15,34]

In the present study, evaluation of tissue compatibility was based on detection of two markers in the whole brain coronal section: GFAP and Iba-1, which are increasingly expressed in reactive astrocytes and activated microglia, respectively. Generally, when a foreign body is introduced into the brain, Iba-1-positive microglia cells can be observed within the site of implantation of the foreign body within a very short time frame following placement; then, the GFAP-positive reactive astrocytes are recruited to the foreign body, eventually encapsulate it with a glial scar if the foreign body is not degradable or degrades very slowly.[35] In the present study, the injected UBM material did not elicit an adverse immune reaction in rat brains as evidenced by the degree to which, microglia and astrocyte activation were found to be similar to PBS injection. No glial scarring was found at the site of injection suggesting a fast degradation rate of the UBM and further suggesting that UBM modulates the host tissue response to prevent glial scarring.

Tissue compatibility of UBM was also evaluated by Fluorojade B staining to detect degenerated or dead neurons

around the injection site. Fluorojade B is a high-affinity fluorescent marker for the localization of neuronal degeneration.[36] Few dead neurons were observed near or within the injection site in the UBM group or PBS group. Previous studies have shown that ECM materials do not exhibit any toxic effects upon various tissues, such as artery, skin, urinary tract, tendon, and ligament.[13] This study provides the first direct evidence that a hydrogel preparation composed of UBM-ECM does not have cytotoxic effects upon neurons in the brain. Together with the mild inflammatory response and lack of scarring, the UBM hydrogel demonstrated excellent biocompatibility within the brain tissue.

It has been shown that ECM scaffolds contain growth factors, which are released during scaffold degradation. Among them, FGF-2 is capable of promoting neurogenesis and reducing cell degeneration in the granule cell layer of the hippocampus,[37] while TGF-β has been shown to modulate inflammatory reactions in the injured brain.[38] Other growth factors could also contribute to the neuroprotection effects, including VEGF, EGF, FGF, TGF-β, HGF, among others, which are beneficial for phenomena such as angiogenesis, mitogenesis, and the resolution of inflammation.[13] While the specific amounts or activity of growth factors present in the ECM, which was used in this study, were not investigated or determined, materials were produced in a manner identical to previous studies demonstrating maintenance of such factors. Small molecules and bioactive peptides derived from degradation products of the ECM have also been shown to exert chemotaxic and mitogenic effects on endogenous progenitor or stem cell populations.[19,39,40] While not examined in the present study, these cells may have been recruited to the site or promoted to proliferate by UBM, and they may then provide a potential trophic mechanism for the observed repair of the circuit of neurons for motor function. The reduced lesion volume, lessened white matter injury, as well as the improved vestibulomotor function recovery by UBM in our study may be the result of one or more of the above mechanisms. However, additional studies will be required to determine the exact mechanisms by which ECM scaffold materials are capable of promoting functional recovery following injection into injured brain tissues.

In the present study, UBM hydrogel injection did not prevent the cell loss in CA3. Interestingly, UBM treatment also failed to improve cognitive function. Since cognitive deficits after TBI are thought to be a result of neuronal loss in CA3 of hippocampus, this may explain the lack of improvement on cognitive functions. However, it remains indeterminate if this is a causal phenomenon. Further, the ideal postinjury time of injection has not yet been determined, and may affect outcomes in future studies.

Most recently, the matrix from CNS has also been isolated from the porcine brain, spinal cord, and optic nerve.[15] An *in vitro* study proved that the matrix from CNS compared with UBM promoted PC12 cell migration, not the rate of differentiation. These isolated CNS forms of the ECM have comparable amount of VEGF and bFGF to UBM-ECM. The matrix from the optic nerve contains NGF, which indicates that the matrix from CNS may provide more tissue-specific cues to aid functional recovery after CNS injury. However, the matrix from CNS was not investigated in the present study and should be examined in future studies.[15]

Conclusion

The present study demonstrated that UBM is very well-tolerated by the brain tissue and has positive effects upon the injured brain tissue and motor function recovery following experimentally induced TBI in rats. Importantly, the reduced tissue injury and some functional recovery were attained without the administration of exogenously derived stem cells. These findings suggest that the UBM hydrogel may be of therapeutic benefit for TBI. On the other hand, the cell loss and cognitive deficit were not prevented by UBM treatment alone, indicating that exogenous cell transplantation may still be necessary. Along this line, UBM may be an ideal scaffold material for stem cell transplantation in future studies aiming at full functional recovery after TBI.

Acknowledgments

We acknowledge the financial support provided by the Department of Defense Concept Award PT073219 (J.C.), NSF Career Award 0748001 (X.T.C.).

Disclosure Statement

No competing financial interests exist.

References

1. VA Research and Development Leading in the 21st Century. Available at www.research.va.gov/researchweek/press_packet/leading21st-century.pdf
2. Faul, M., *et al.* Using a cost-benefit analysis to estimate outcomes of a clinical treatment guideline: testing theBrain Trauma Foundation guidelines for the treatment of severe traumatic brain injury. J Trauma **63,** 1271, 2007.
3. Ray, S.K., Dixon, C.E., and Banik, N.L. Molecular mechanisms in the pathogenesis of traumatic brain injury. Histol Histopathol **17,** 1137, 2002.
4. Gage, F.H., *et al.* Survival and differentiation of adult neuronal progenitor cells transplanted to the adult brain. Proc Natl Acad Sci U S A **92,** 11879, 1995.
5. Gao, J., *et al.* Transplantation of primed human fetal neural stem cells improves cognitive function in rats after traumatic brain injury. Exp Neurol **201,** 281, 2006.
6. Hoane, M.R., *et al.* Transplantation of neuronal and glial precursors dramatically improves sensorimotor function but not cognitive function in the traumatically injured brain. J Neurotrauma **21,** 163, 2004.
7. Woerly, S., Marchand, R., and Lavallee, C. Intracerebral implantation of synthetic polymer/biopolymer matrix: a new perspective for brain repair. Biomaterials **11,** 97, 1990.
8. Menei, P., *et al.* Biodegradation and brain tissue reaction to poly(D,L-lactide-co-glycolide) microspheres. Biomaterials **14,** 470, 1993.
9. Liu, C.Y., Apuzzo, M.L., and Tirrell, D.A. Engineering of the extracellular matrix: working toward neural stem cell programming and neurorestoration—concept and progress report. Neurosurgery **52,** 1154; discussion 1165, 2003.
10. Tate, C.C., *et al.* Laminin and fibronectin scaffolds enhance neural stem cell transplantation into the injured brain. J Tissue Eng Regen Med **3,** 208, 2009.
11. Badylak, S.F. The extracellular matrix as a biologic scaffold material. Biomaterials **28,** 3587, 2007.
12. Marcal, H., *et al.* A comprehensive protein expression profile of extracellular matrix biomaterial derived from porcine urinary bladder. Regen Med **7,** 159, 2012.

13. Badylak, S.F. Xenogeneic extracellular matrix as a scaffold for tissue reconstruction. Transpl Immunol **12,** 367, 2004.
14. Hodde, J.P., and Hiles, M.C. Bioactive FGF-2 in sterilized extracellular matrix. Wounds **13,** 195, 2001.
15. Crapo, P.M., *et al.* Biologic scaffolds composed of central nervous system extracellular matrix. Biomaterials **33,** 3539, 2012.
16. Brown, B., *et al.* The basement membrane component of biologic scaffolds derived from extracellular matrix. Tissue Eng **12,** 519, 2006.
17. Agrawal, V., *et al.* Evidence of innervation following extracellular matrix scaffold-mediated remodelling of muscular tissues. J Tissue Eng Regen Med **3,** 590, 2009.
18. Freytes, D.O., *et al.* Preparation and rheological characterization of a gel form of the porcine urinary bladder matrix. Biomaterials **29,** 1630, 2008.
19. Zantop, T., *et al.* Extracellular matrix scaffolds are repopulated by bone marrow-derived cells in a mouse model of achilles tendon reconstruction. J Orthop Res **24,** 1299, 2006.
20. Ortuzar, N., *et al.* Combination of intracortically administered VEGF and environmental enrichment enhances brain protection in developing rats. J Neural Transm **118,** 135, 2011.
21. Makwana, M., *et al.* Endogenous transforming growth factor beta 1 suppresses inflammation and promotes survival in adult CNS. J Neurosci **27,** 11201, 2007.
22. Dixon, C.E., *et al.* A controlled cortical impact model of traumatic brain injury in the rat. J Neurosci Methods **39,** 253, 1991.
23. Yan, H.Q., *et al.* Evaluation of combined fibroblast growth factor-2 and moderate hypothermia therapy in traumatically brain injured rats. Brain Res **887,** 134, 2000.
24. Chen, J., *et al.* Atorvastatin induction of VEGF and BDNF promotes brain plasticity after stroke in mice. J Cereb Blood Flow Metab **25,** 281, 2005.
25. Swanson, R.A., *et al.* A semiautomated method for measuring brain infarct volume. J Cereb Blood Flow Metab **10,** 290, 1990.
26. Irving, E.A., Bentley, D.L., and Parsons, A.A. Assessment of white matter injury following prolonged focal cerebral ischaemia in the rat. Acta Neuropathol **102,** 627, 2001.
27. Hamm, R.J., *et al.* Cognitive deficits following traumatic brain injury produced by controlled cortical impact. J Neurotrauma **9,** 11, 1992.
28. Daly, K.A., *et al.* Effect of the alpha gal epitope on the response to small intestinal submucosa extracellular matrix in a nonhuman primate model. Tissue Eng Part A **15,** 3877, 2009.
29. Brown, B.N., *et al.* Macrophage phenotype and remodeling outcomes in response to biologic scaffolds with and without a cellular component. Biomaterials **30,** 1482, 2009.
30. Brown, B.N., *et al.* Macrophage phenotype as a predictor of constructive remodeling following the implantation of biologically derived surgical mesh materials. Acta Biomater **8,** 978, 2012.
31. Schwartz, M. "Tissue-repairing" blood-derived macrophages are essential for healing of the injured spinal cord: from skin-activated macrophages to infiltrating blood-derived cells? Brain Behav Immun **24,** 1054, 2010.
32. Lazarov-Spiegler, O., *et al.* Restricted inflammatory reaction in the CNS: a key impediment to axonal regeneration? Mol Med Today **4,** 337, 1998.
33. Lazarov-Spiegler, O., *et al.* Transplantation of activated macrophages overcomes central nervous system regrowth failure. FASEB J **10,** 1296, 1996.
34. DeQuach, J.A., *et al.* Decellularized porcine brain matrix for cell culture and tissue engineering scaffolds. Tissue Eng Part A **17,** 2583, 2011.
35. Polikov, V.S., Tresco, P.A. and Reichert, W.M. Response of brain tissue to chronically implanted neural electrodes. J Neurosci Methods **148,** 1, 2005.
36. Schmued, L.C., and Hopkins, K.J. Fluoro-Jade B: a high affinity fluorescent marker for the localization of neuronal degeneration. Brain Res **874,** 123, 2000.
37. Yoshimura, S., *et al.* FGF-2 regulates neurogenesis and degeneration in the dentate gyrus after traumatic brain injury in mice. J Clin Invest **112,** 1202, 2003.
38. Basu, A., *et al.* Transforming growth factor beta1 prevents IL-1beta-induced microglial activation, whereas TNFalpha- and IL-6-stimulated activation are not antagonized. Glia **40,** 109, 2002.
39. Brennan, E.P., *et al.* Chemoattractant activity of degradation products of fetal and adult skin extracellular matrix for keratinocyte progenitor cells. J Tissue Eng Regen Med **2,** 491, 2008.
40. Marra, K.G., *et al.* FGF-2 enhances vascularization for adipose tissue engineering. Plast Reconstr Surg **121,** 1153, 2008.

Address correspondence to:
Xinyan Tracy Cui, PhD
Department of Bioengineering
University of Pittsburgh
Pittsburgh, PA 15261

E-mail: xic11@pitt.edu

Jun Chen, MD, PhD
Department of Neurology
Center of Cerebrovascular Disease Research
University of Pittsburgh School of Medicine
Pittsburgh, PA 15261

E-mail: chenj2@upmc.edu

Received: October 22, 2012
Accepted: March 19, 2013
Online Publication Date: May 27, 2013